Impact of the Intraseasonal Variability of the Western North Pacific Large-Scale Circulation on Tropical Cyclone Tracks

TSING-CHANG CHEN AND SHIH-YU WANG

Atmospheric Science Program, Department of Geological and Atmospheric Sciences, Iowa State University, Ames, Iowa

MING-CHENG YEN

Department of Atmospheric Science, National Central University, Chung-Li, Taiwan

ADAM J. CLARK

Atmospheric Science Program, Department of Geological and Atmospheric Sciences, Iowa State University, Ames, Iowa

(Manuscript received 15 July 2008, in final form 25 October 2008)

ABSTRACT

The life cycle of the Southeast Asian–western North Pacific monsoon circulation is established by the northward migrations of the monsoon trough and the western Pacific subtropical anticyclone, and is reflected by the intraseasonal variations of monsoon westerlies and trade easterlies in the form of an east–west seesaw oscillation. In this paper, an effort is made to disclose the influence of this monsoon circulation on tropical cyclone tracks during its different phases using composite charts of large-scale circulation for certain types of tracks.

A majority of straight-moving (recurving) tropical cyclones appear during weak (strong) monsoon westerlies and strong (weak) trade easterlies. The monsoon conditions associated with straight-moving tropical cyclones are linked to the intensified subtropical anticyclone, while that associated with recurving tropical cyclones is coupled with the deepened monsoon trough. The relationship between genesis locations and track characteristics is evolved from the intraseasonal variation of the monsoon circulation reflected by the east–west oscillation of monsoon westerlies and trade easterlies. Composite circulation differences between the flows associated with the two types of tropical cyclone tracks show a vertically uniform short wave train along the North Pacific rim, as portrayed by the Pacific–Japan oscillation. During the extreme phases of the monsoon life cycle, the anomalous circulation pattern east of Taiwan resembles this anomalous short wave train.

A vorticity budget analysis of the strong monsoon condition reveals a vorticity tendency dipole with a positive zone to the north and a negative zone to the south of the deepened monsoon trough. This meridional juxtaposition of vorticity tendency propagates the monsoon trough northward. The interaction of a tropical cyclone with the monsoon trough intensifies the north–south juxtaposition of the vorticity tendency and deflects the tropical cyclone northward. In contrast, during weak monsoon conditions, the interaction between a tropical cyclone and the subtropical high results in a northwestward motion steered by the intensified trade easterlies. The accurate prediction of the monsoon trough and the subtropical anticyclone variations coupled with the monsoon life cycle may help to improve the forecasting of tropical cyclone tracks.

1. Introduction

The summer monsoon circulation in East and Southeast Asia is composed of the monsoon trough stretching from northern Indochina to the Philippine Sea, the western North Pacific anticyclone, and the mei-yu–baiu rainband. Sequential passages of the mei-yu–baiu rainband in early summer, the western Pacific anticyclone in midsummer, and the tropical cyclone activity in late summer form the life cycle of the East and Southeast Asian monsoon (Chen et al. 2004). Because of this northward progression of these circulation elements, there is a phase lag of a monsoon life cycle between the southern (e.g., Hong Kong and Taiwan) and northern (e.g., Korea and Japan) regions of East Asia. This phase lag is reflected by a distinct opposite-phase intraseasonal

Corresponding author address: Tsing-Chang (Mike) Chen, Atmospheric Science Program, Dept. of Geological and Atmospheric Sciences, 3010 Agronomy Hall, Iowa State University, Ames, IA 50011.
E-mail: tmchen@iastate.edu

DOI: 10.1175/2008WAF2222186.1

oscillation of monsoon circulation cells between these two regions (Chen et al. 2000). This oscillation is caused by the northward migration of the 30–60-day mode monsoon trough–ridge system (e.g., Krishnamurti and Subrahmanyam 1982; Chen and Chen 1995) coupled with the eastward-propagating global 30–60-day mode (Madden and Julian 1971, 1972). Over the western tropical Pacific and tropical Southeast Asia, this coupling also leads to the intraseasonal oscillations of monsoon westerlies and trade easterlies. Because tropical cyclones are steered primarily by the large-scale environmental flow (e.g., Chan and Gray 1982; Holland 1983), it is likely that the characteristics of tropical cyclone tracks in the western North Pacific are modulated by the northward progression of the monsoon circulation elements in Southeast and East Asia and also reflected by the intraseasonal oscillation of this monsoon circulation within the context of the monsoon life cycle.

Over several typhoon seasons, Harr and Elsberry (1991) observed that tropical cyclone tracks alternate between clusters of straight and recurving paths with an intraseasonal time scale. This characteristic of tropical cyclone tracks is possibly established by the intraseasonal variations of the monsoon circulation over the western North Pacific. To support this suggestion, composite 700-mb anomalous circulation patterns associated with straight, recurving-south (formed south of 20°N), and recurving-north (formed north of 20°N) tropical cyclone tracks, and inactive periods of tropical cyclone activity were constructed. The first two types of tracks are associated with anomalous cyclonic circulations that deepen the monsoon trough in the western tropical Pacific. In contrast, the last two types of tracks are linked to the weakened subtropical ridge by an anomalous anticyclonic circulation. These anomalous circulation patterns were constructed based on the types of tropical cyclone tracks. Thus, it is not clear how the anomalous circulation is transferred from one track type to the other.

To explore the transition between anomalous circulation patterns of different types of tropical cyclone tracks, Harr and Elsberry (1995a,b) used the empirical orthogonal function and cluster analysis, and identified six large-scale variations or patterns of the monsoon trough and subtropical ridge, independent of tropical cyclone track characteristics. Transitions are most likely to occur between the recurrent patterns associated with the active monsoon trough and the inactive monsoon condition. Relating tropical cyclone motion to the monsoon trough from a synoptic perspective, Lander (1996) observed that tropical cyclones tend to move northwestward when the axis of the monsoon trough is oriented along its climatological NW–SE direction. On the other hand, tropical cyclones within the monsoon trough tend to move northward when the monsoon trough becomes reverse (SW–NE) oriented. The reverse-oriented monsoon trough occurs roughly once in every June–September typhoon season.

It was suggested by previous studies that anomalous circulation patterns associated with different types of tropical cyclone tracks and the orientation reversal of the monsoon trough are likely formed by the interaction of the Asia monsoon circulation with the eastward-propagating 30–60-day mode. However, this link has not been well established and anomalous circulation patterns were basically formed in terms of track types. In fact, the modulation of the monsoon circulation by the intraseasonal mode is often depicted by the circulation at different phases of the monsoon circulation defined by various monsoon indices (e.g., rainfall or surface wind at a specific area). To enhance our understanding of the impact of the 30–60-day monsoon mode on the tropical cyclone motion, it is more useful to explore the characteristics of tropical cyclone tracks embedded in the monsoon circulation during different phases of the 30–60-day mode.

For the circulation analysis, this study employed the 40-yr European Centre for Medium-Range Weather Forecasts (ECMWF) Re-Analysis (ERA-40) global reanalyses with a spatial resolution of 2.5° × 2.5° (Uppala et al. 2005). For tropical cyclones in the western North Pacific, tropical cyclone track records from the Joint Typhoon Warning Center (JTWC) in Hawaii were used. The analysis period covers June–October and spans from 1979 to 2004. Because the ERA-40 reanalyses are only available up to 2002, the years of 2003–04 were analyzed using the National Centers for Environmental Prediction–Department of Energy (NCEP–DOE) Global Reanalysis 2 for 2003–06 (Kanamitsu et al. 2002).

This research effort is preceded by an analysis for the modulation of the 30–60-day mode on tropical cyclone tracks during 1996 in section 2. To generalize findings obtained in section 2, two composite analysis approaches are performed in section 3: composite flow patterns of recurving and straight-moving tropical cyclone tracks in section 3a, and composite 30–60-day bandpass-filtered flow patterns and their associated tropical cyclone tracks in section 3b. A vorticity budget analysis for exploring the dynamics involved with the change in the tropical cyclone track is pursued in section 4. Concluding remarks are provided in section 5.

2. MJO modulation on tropical cyclone tracks: 1996

To illustrate the possible effects of the intraseasonal variabilities of the Southeast Asian monsoon and the western North Pacific anticyclone on the characteristics

of tropical cyclone tracks, the longitude–time (x–t) diagram of the 850-hPa zonal wind at 15°N for the period of July–October 1996 is shown in Fig. 1, from which the intraseasonal variabilities clearly emerge. However, a more precise measurement for the intraseasonal variation of monsoon westerlies can be obtained by imposing the 30–60-day bandpass-filtered 850-hPa zonal wind, $\tilde{u}$(850 hPa), at (15°N, 115°E) on the x–t diagram of u(850 hPa). Although monsoon rainfall has been used as an operational parameter to define the strength and life cycle of a monsoon, the monsoon westerlies are often adopted as an index to depict the intensity variation of the monsoon circulation (e.g., Krishnamurti and Subrahmanyam 1982; Chen and Chen 1995). This $\tilde{u}$(850 hPa) index is constructed using the 30–60-day second-order Butterworth bandpass filter (Murakami 1979). Regardless of the existence of other higher-frequency signals, two cycles of the 30–60-day oscillation of monsoon westerlies dominate during this tropical cyclone season. When the monsoon westerlies become strong (i.e., a strong monsoon) and expand eastward, the trade easterlies appear to be weak and retreat eastward, while the reverse contrast occurs when the monsoon becomes weak.

The superposition of all tropical cyclones south of 25°N (22 of 27 total western North Pacific tropical cyclones during 1996), according to their longitudes in Fig. 1, reveals that straight-moving tropical cyclones occur with the inactive monsoon trough, and recurving tropical cyclones occur with the active monsoon trough. The methodology used to define tropical cyclone tracks is described in the appendix. To observe synoptically the coupling of the east–west intraseasonal seesaw oscillation between monsoon westerlies and trade easterlies with the northward migrations of the monsoon trough and the subtropical anticyclone, the transition period from strong trade easterlies to strong monsoon westerlies that occurred on 4–16 September 1996 (marked by a red-dashed oval in Fig. 1) is analyzed in terms of the evolution of the 850-hPa streamline charts superimposed with isotachs, and locations and tracks of tropical cyclones (Fig. 2). During 4–8 September 1996 (Figs. 2a–c), the trade easterlies along the southern periphery of the subtropical anticyclone and the northern side of the monsoon trough became stronger. The monsoon trough over the South China Sea moved northward from south of the Mekong Delta on 4 September to east of Hailan Island. The ridge line located from across southern Japan to the ocean south of the Aleutian Islands moved to northern Japan and eastward. Typhoon Sally (No. 1) and Tropical Depression 24 (TD24, No. 2) were steered by strong trade easterlies of the subtropical anticyclone with straight

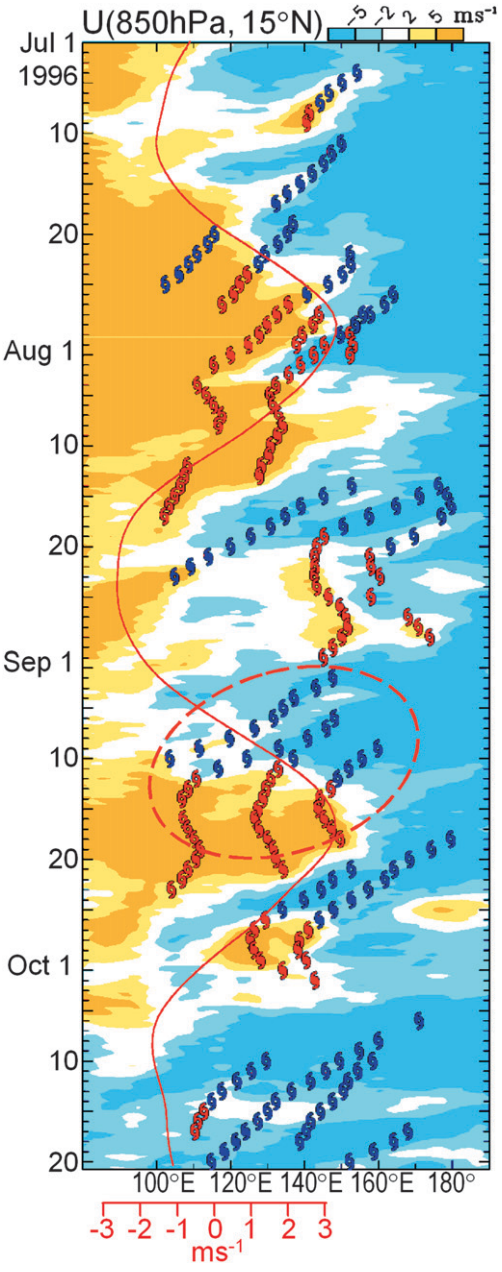

FIG. 1. Longitude–time (x–t) diagram of the 850-hPa zonal wind (U) at 15°N superimposed with the longitudinal positions of tropical cyclones (typhoon symbols) at 0000 UTC formed within the latitudinal zone of 0°–25°N. The corresponding typhoon symbols are colored in red (blue) when the propagation direction of the tropical cyclones is smaller than 45° away from the west in the second quadrant (45° away from the east in the first quadrant). The 30–60-day bandpass-filtered 850-hPa zonal wind at (15°N, 115°E) ($\tilde{U}$) (red line) is used as a monsoon index. The red-dashed oblong around 10 September indicates that the 850-hPa environmental flow embedded by tropical cyclones appearing within the time period indicated by this oblong will be illustrated in Fig. 3.

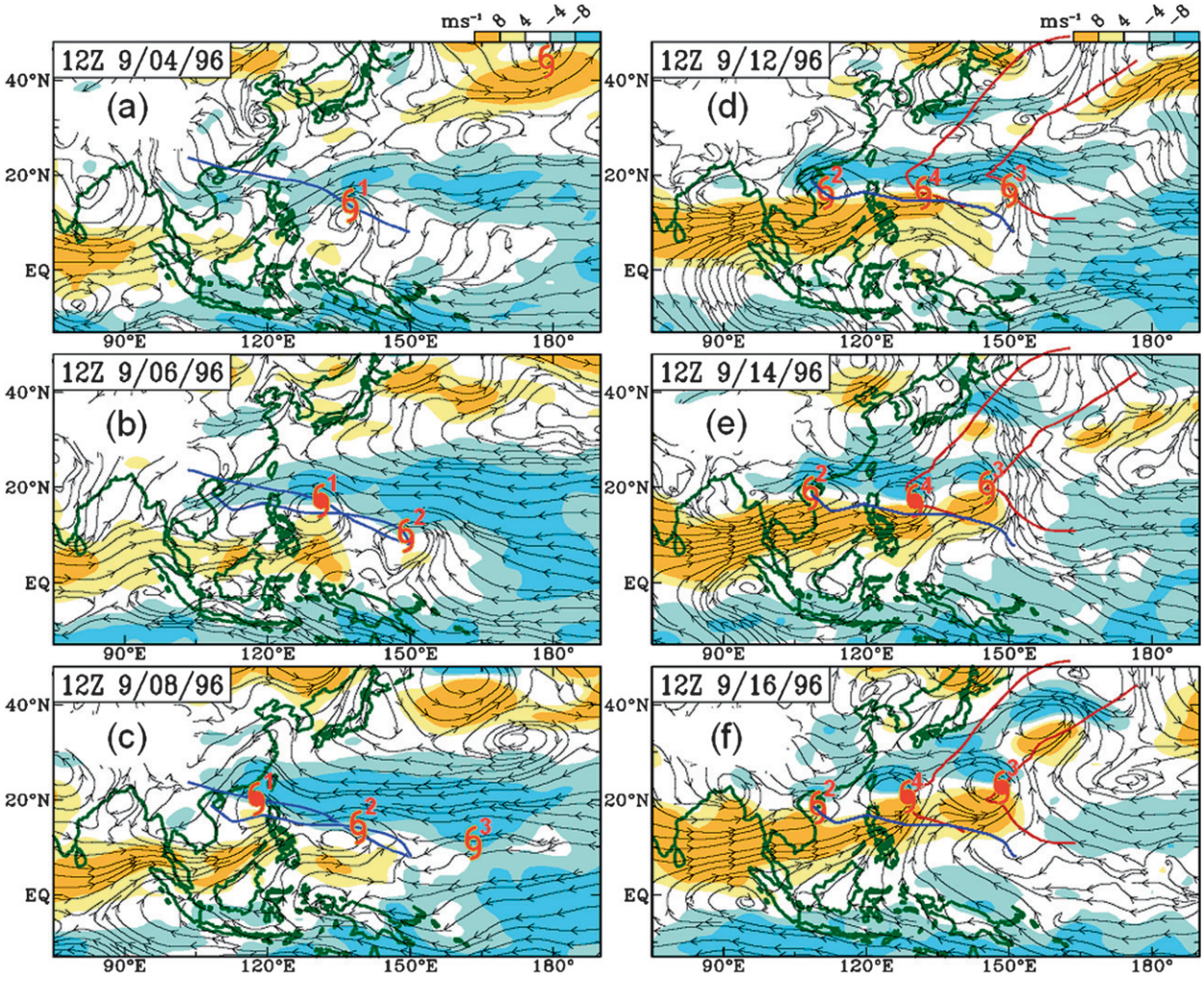

FIG. 2. The 850-hPa streamlines and zonal wind (shadings) at 1200 UTC on (a) 4, (b) 6, (c) 8, (d) 12, (e) 14, and (f) 16 Sep 1996 superimposed with four tropical cyclones: Sally (1), TD 24 (2), Tom (3), and Violet (4). Tropical cyclones with sustained wind speeds >(≤)64 kt are marked by solid (open) typhoon symbols, while straight (recurving) tropical cyclone tracks are indicated by blue (red) solid lines.

tracks. At the end of this time period, two more typhoons, Tom (No. 3) and Violet (No. 4), formed on 8 and 9 September, respectively.

The monsoon trough was oriented NW–SE on 8 September (Fig. 2c). On 12 September, the monsoon trough became oriented E–W (Fig. 2d). The northward migration of the east side of the monsoon trough was accompanied by the eastward retreat of the subtropical anticyclone, the weakening of easterlies north of the monsoon trough, and the strengthening of the monsoon westerlies. On 16 September, the monsoon trough became oriented SW–NE [or reverse oriented as described by Lander (1996)]. The monsoon westerlies became stronger and the easterlies north of the monsoon trough appeared weaker. Thus, the eastward retreat of the western subtropical anticyclone allowed Typhoons Tom and Violet to be deflected northward and to recurve within the reverse-oriented monsoon trough. From this example it appears that the characteristics of tropical cyclone tracks and the intensity difference between monsoon westerlies and trade easterlies may be correlated.

To confirm that such a correlation can be applied to the majority of tropical cyclones in the western North Pacific, 26 typhoon seasons (1979–2004) are analyzed. Time series of the previously defined $\tilde{u}$(850 hPa) index during every typhoon season from 1979 to 2004 are shown in Fig. 3, superimposed with tropical cyclones that formed south of 25°N [345 of 426 (81%) western North Pacific tropical cyclones]. Because the cycles of the $\tilde{u}$(850 hPa) index in every typhoon season are not always in phase, these indices are aligned so that the

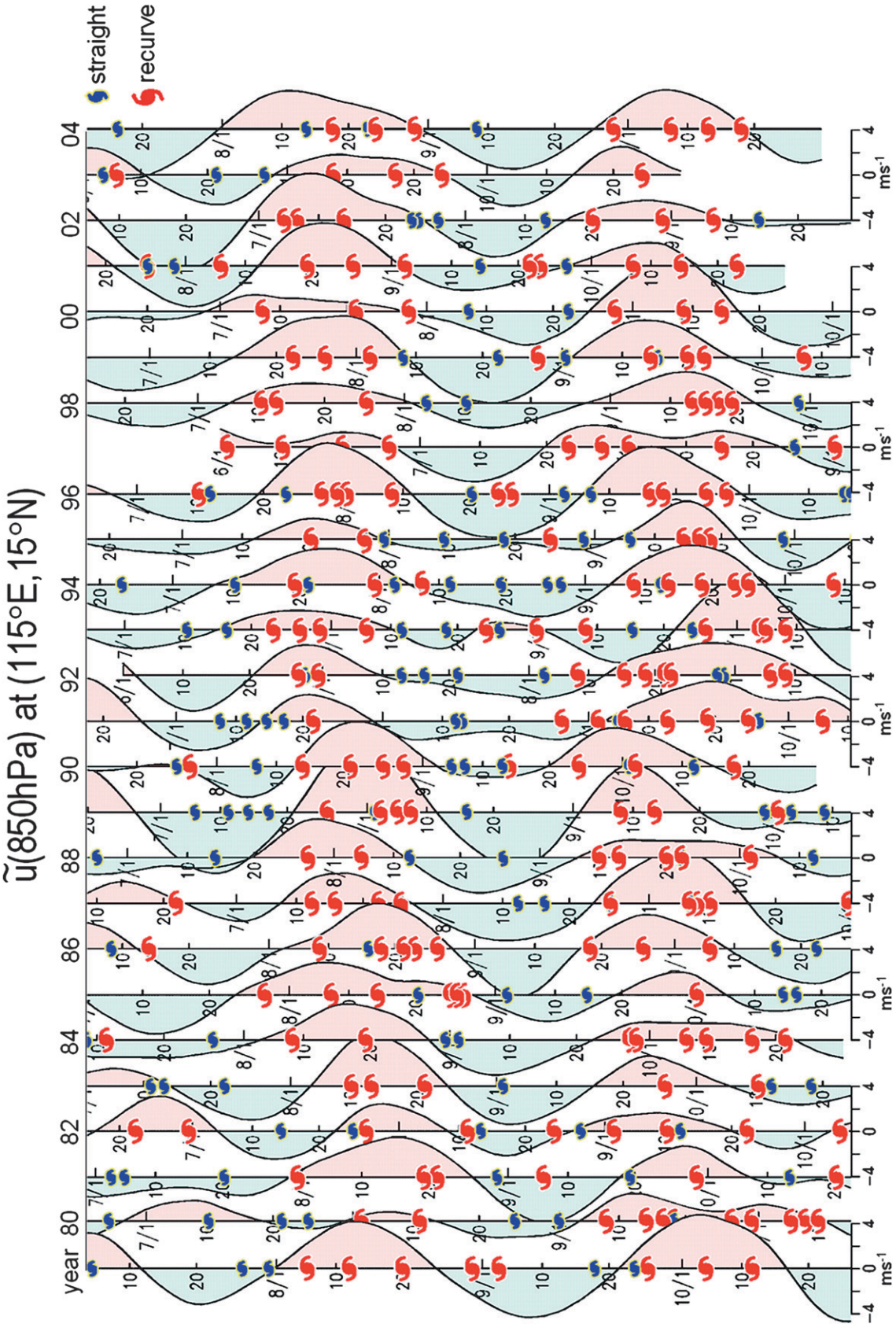

FIG. 3. Following Fig. 1, time series of 30–60-day bandpass-filtered 850-hPa zonal winds ($\tilde{u}$) at (15°N, 115°E) superimposed with typhoons during their midlife within the latitudinal zone of 0°–25°N, for 26 typhoon seasons (1979–2004). Straight-moving (recurving) tropical cyclones are marked by blue (red) typhoon symbols. The same phases of the $\tilde{u}$(850 hPa) index of every typhoon season are aligned. The year of each typhoon season is indicated at the top of every other time series of the $\tilde{u}$(850 hPa) index.

maximum and minimum phases are coincident. Aligning the phases from each time series reveals that a great majority of the recurving tropical cyclones occur during monsoon westerly anomalies, while the majority of straight-moving tropical cyclones occur during easterly anomalies, and that this relationship is applicable to every typhoon season.

3. Composite analysis

To identify the flow patterns favorable for different tropical cyclone tracks and to explore the possible relationship between upper- and lower-level flows for these tracks, composite flow patterns for recurving and straight tropical cyclone tracks at the midpoint of the tropical cyclone life cycle (referred to hereafter as midlife) are analyzed in this section. In addition, to examine how the characteristics of tropical cyclone activity are changed by the transition of the large-scale circulation from strong to weak monsoons (or vice versa), composites of the 30–60-day monsoon circulation anomalies during different phases of the monsoon life cycle are presented. A special effort is made to relate the transition of monsoon flow patterns within the context of the monsoon life cycle.

a. Composite flow patterns associated with recurving and straight-moving tropical cyclone tracks

The flows associated with tropical cyclones that have a midlife location within the region (10°–30°N, 115°–155°E) are used for composites. Composite 300- and 850-hPa streamline charts associated with recurving and straight-moving tropical cyclones at their midlife are shown in Fig. 4 with average tracks of recurving and straight-moving tropical cyclones superimposed. Approximately 95% of 426 tropical cyclones during the 1979–2004 period are included in this composite procedure, and the procedure for constructing average tropical cyclone tracks is explained in the appendix.

The upper-tropospheric flow patterns associated with recurving and straight tropical cyclone tracks in Figs. 4a and 4c, respectively, resemble those observed by Chen and Ding (1979). The upper-level trough separating the Tibetan anticyclone and the western subtropical Pacific anticyclone deflects tropical cyclones northward. The merger of these anticyclones steers tropical cyclones approximately straight west. At 850 hPa, the monsoon westerlies are stronger for the recurving track than for the straight track (Fig. 4b), while the trade easterlies are stronger for the straight track than for the recurving track (Fig. 4d). This feature is consistent with that shown in Figs. 1–3. In addition to the contrast between monsoon westerlies and trade easterlies, the monsoon trough and the subtropical anticyclone are farther north for the recurving track than for the straight track. For the straight track (Fig. 4d), the eastern portion of the monsoon trough is anchored east of the Philippines, and the western portion of the ridge line of the subtropical anticyclone is located at the Yangtze River. For the recurving track (Fig. 4b), the monsoon trough migrates northward to the ocean east of the Luzon Strait and the ridge line migrates northward to northern China.

It is not immediately clear how the upper- and lower-tropospheric flows are related to each other for each type of tropical cyclone track shown in Fig. 4; thus, to illustrate this relationship, the streamline charts of the flow differences between the two types of tracks are presented (Figs. 4e and 4f). A short wave train emerges along the northwestern rim of the northwest Pacific. Despite the structure of the monsoon circulation in Southeast–East Asia, the short wave trains at the upper and lower troposphere resemble each other, forming a *barotropic* or vertically uniform structure.[1] For the recurving tracks, the anomalous cyclonic circulation around Taiwan is meridionally juxtaposed with anomalous anticyclonic circulations to its south and north. The anomalous westerlies between Taiwan and the Philippines hinder the northwestward propagation of tropical cyclones, while the anomalous cyclonic circulation around Taiwan deflects tropical cyclones northward. For straight-moving tropical cyclones, the spatial structure of the short wave train shown in Figs. 4e and 4f is reversed (not shown). The anomalous easterlies through the Luzon Strait facilitate the westward propagation of tropical cyclones.

The barotropic characteristic of the aforementioned short wave train is a crucial feature that can be used to verify whether numerical forecasts of tropical cyclones with different tracks have the corresponding large-scale flow patterns that match the observations. In addition, because the spatial structure of this short wave train resembles that of the North Pacific–Japan oscillation (PJO) in response to the summer sea surface temperature anomalies over the tropical Pacific (Nitta 1987), the characteristics of tropical cyclone tracks in the western North Pacific likely undergo an interannual variation through the modulation of the PJO. Currently being investigated, this possibility will be reported upon in the near future.

[1] The vertical structure of monsoon circulation exhibits a phase change. The spatial structure of the two circulation cells south of Japan is revealed at 200 hPa, a characteristic of monsoon circulation. For this reason, the anomalous circulation is depicted by the 850- and 300-hPa streamline charts.

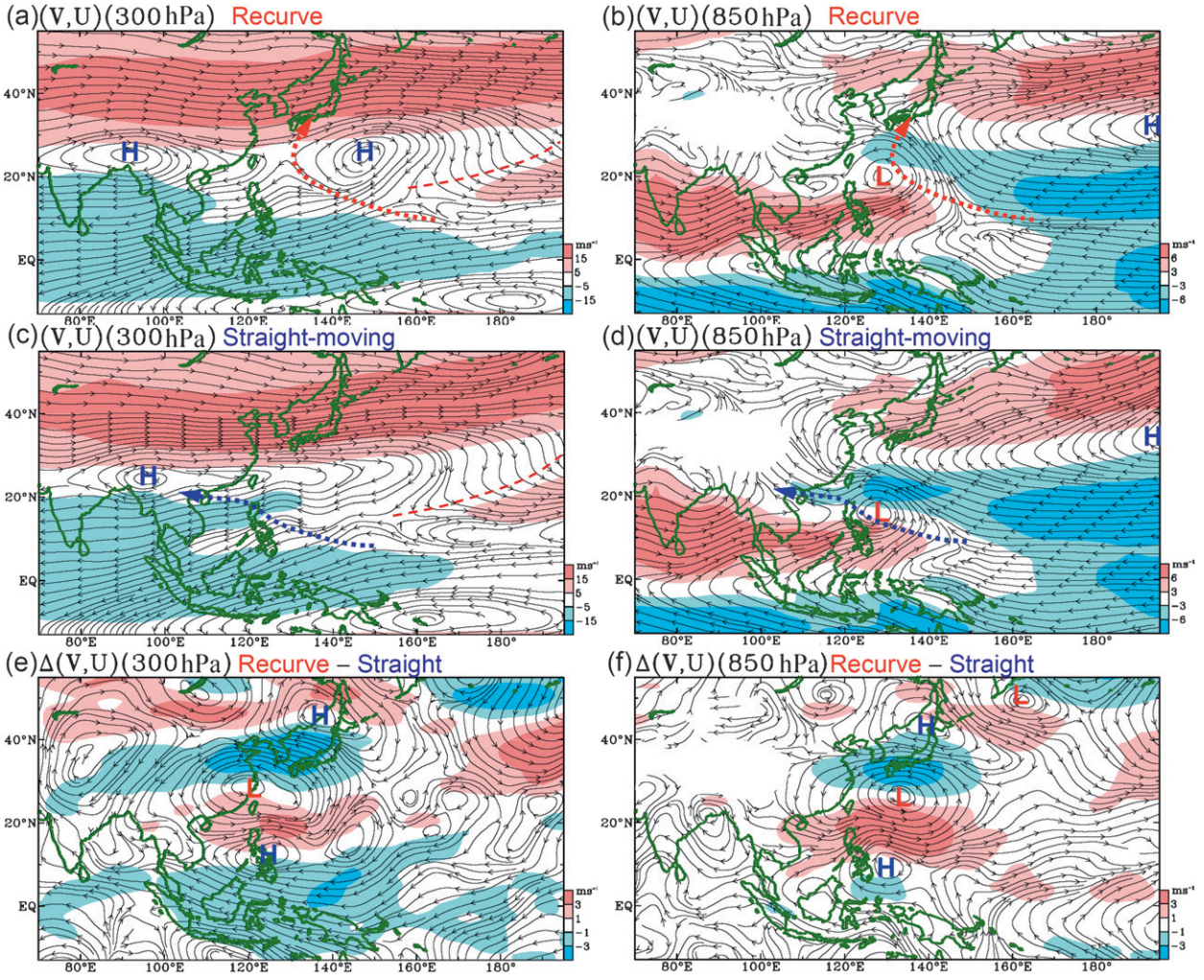

FIG. 4. Composite streamline charts superimposed with zonal wind speeds at (a) 300 and (b) 850 hPa, averaged when the midlife positions of recurving typhoons are located within the region (10°–30°N, 115°–155°E). (c),(d) As in (a),(b) except for straight-moving tropical cyclones. Differences are between composite streamlines of recurving and straight-moving tropical cyclones at (e) 300 and (f) 850 hPa. The mean trajectories of recurving and straight-moving typhoons indicated as thick red and blue dotted arrow lines are added in (a),(b) and (c),(d), respectively. The oceanic trough line is marked by a red-dashed line. The cyclonic (anticyclonic) centers are denoted by red Ls (blue Hs).

Although the PJO is a regional climate mode in the western North Pacific, Nitta (1987) showed that the PJO is linked to a short wave train that extends around the northern rim of the North Pacific. Composite streamline differences in Fig. 5, which are expanded to cover the entire North Pacific basin, show that the short wave trains revealed from the differences in the streamlines between recurving and straight tracks of tropical cyclones extend through the same region. Examining whether this cross–North Pacific short wave train has any impacts on the summer weather system around the North Pacific rim, the North American continent, and beyond will be a challenge for future research.

b. Composite 30–60-day flow patterns and associated tropical cyclone tracks

It was pointed out in section 1 that the evolution of the monsoon circulation results from northward progressions of the monsoon trough, the subtropical anticyclone, and the mei-yu–baiu rainbelt in combination with the 30–60-day monsoon mode. This relationship can be revealed from the comparison between the *y–t* diagrams of u(850 hPa) and $\tilde{u}$(850 hPa) at 135°E during the summer of 1996 (corresponding to Fig. 1) in Fig. 6. During the 1996 tropical cyclone season, both monsoon westerlies and trade easterlies have a very coherent

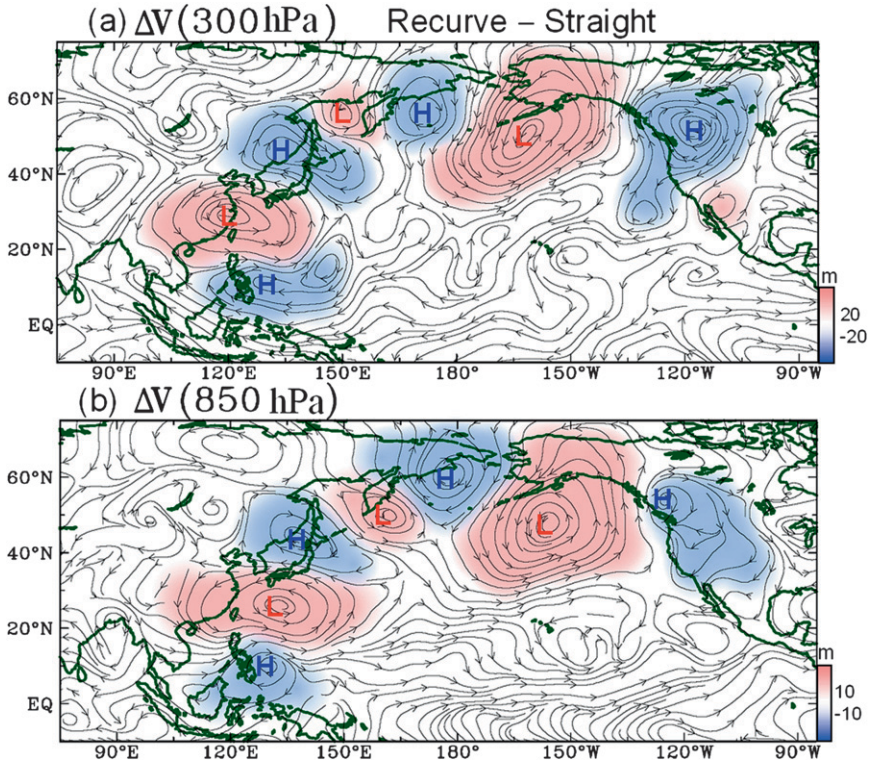

FIG. 5. As in Figs. 4e and f, but for a domain covering the entire North Pacific. Anomalous cyclonic (anticyclonic) circulations associated with the cross-Pacific short wave train are indicated by light pink (blue) shaded areas.

30–60-day oscillation in intensity and east–west intrusion, so that the phase relationship between these two flows with opposite direction is easily distinguishable. This east–west oscillation of tropical zonal winds is also reflected by the alternation between the positive and negative anomalies of u(850 hPa) and $\tilde{u}$(850 hPa). To examine whether intraseasonal oscillations of these two flows are as distinguishable in all 26 tropical cyclone seasons analyzed, the mean westerlies and easterlies of all typhoon seasons (July–October), and the root-mean-square values of 30–60-day filtered westerlies larger than 6 m s^{-1} and easterlies larger than 3 m s^{-1} are displayed with their mean 850-hPa streamlines in Fig. 7a. Based on the two maxima of the rms, two indices are introduced: westerlies averaged over a 5° × 5° region centered at (10°N, 115°E), u_W(850 hPa), and easterlies averaged over another 5° × 5° region centered at (15°N, 165°E), u_E(850 hPa), at the midlife of each tropical cyclone (within a black dashed box in Fig. 7a).

A scatter diagram is shown in Fig. 7b with u_W(850 hPa) as the abscissa and u_E(850 hPa) as the ordinate. Most straight-moving tropical cyclones cluster in the quadrant [u_W(850 hPa) < 0, u_E(850 hPa) < 0], while most recurving tropical cyclones cluster in another quadrant [u_W(850 hPa) > 0, u_E(850 hPa) < 0]. The 95% confidence level of each u-index group (or density function) is indicated by a dashed oval in Fig. 7. The separation line of bivariate normal random variables (von Storch and Zwiers 1999) is given by a red line in Fig. 7 between the u-index density functions of straight-moving and recurving tropical cyclones. The difference between the u_W(850 hPa) and u_E(850 hPa) indices is statistically significant to distinguish the two groups of tropical cyclone tracks. Because the $\tilde{u}$(850 hPa) index is often used to depict the life cycle of the Southeast–East Asian monsoon, it may be more appropriate to present the scatter diagram in terms of $\tilde{u}_W$(850 hPa) and $\tilde{u}_E$(850 hPa), rather than u_W(850 hPa) and u_E(850 hPa). As shown in Fig. 7c, straight-moving tropical cyclones cluster in the quadrant [$\tilde{u}_W$(850 hPa) > 0, $\tilde{u}_E$(850 hPa) > 0], while the recurving tropical cyclones cluster in another quadrant with both indices smaller than zero. These two groups of the $\tilde{u}$ index are as distinctly separated as those in Fig. 7b.

To gain a synoptic perspective on how the 30–60-day monsoon mode affects the characteristics of tropical cyclone tracks, the composite procedure introduced by Knutson and Weickmann (1987), with a slight modification,

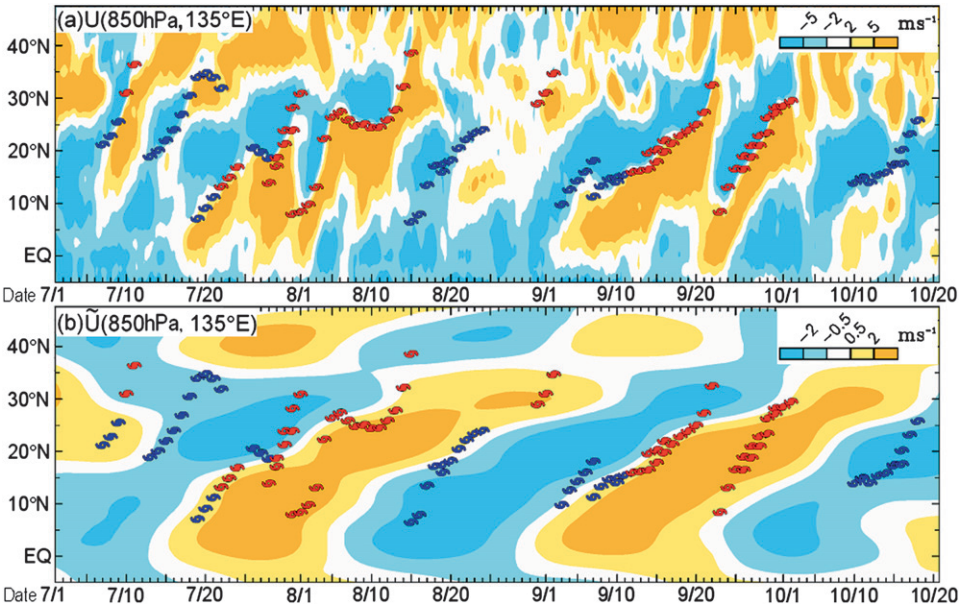

FIG. 6. Latitude–time (y–t) diagrams of (a) 850-hPa total zonal winds (u), and (b) the 30–60-day bandpass-filtered 850-hPa zonal winds ($\tilde{u}$) at 135°E. When their directions changed to the sector between northwest and north, these typhoons are marked by red typhoon symbols, otherwise by dark blue typhoon symbols.

is used. The modified composite analysis is outlined as follows:

1) When the amplitude of the $\tilde{u}_W$(850 h Pa) index at any time during the typhoon season is larger than its average value by at least one standard deviation, the monsoon life cycle (with one trough and one ridge) is selected. If only one-half of the cycle reaches the one standard deviation criterion, this half cycle is used.
2) The entire cycle of the $\tilde{u}_W$(850 hPa) index is evenly divided into eight phases (Fig. 8a). Each phase covers a 5-day period centered on the third day.
3) Tropical cyclones with their midlife occurring within the 5-day period in any one of the eight phases are included in the composite chart of this phase.

The *accumulated* populations of recurving (light gray histogram) and straight-moving (dark gray histogram) tropical cyclones for each phase of the 30–60-day monsoon cycle are shown in Fig. 8b. The largest number of recurving (straight moving) tropical cyclones occurs when the $\tilde{u}_W$(850 hPa) index reaches its maximum (minimum) value, supporting the argument that tropical cyclone tracks are affected by the 30–60-day monsoon mode through the intensity of monsoon westerlies and trade easterlies. Nevertheless, neither track type can be completely excluded in any phase of this intraseasonal monsoon mode.

The ways in which tropical cyclone tracks are affected by the circulation anomalies during different phases of the intraseasonal monsoon mode are illustrated by the 5-day averaged composite of the 30–60-day filtered streamline charts (Fig. 9) superimposed with tracks and midlife locations of corresponding tropical cyclones. The northward migrations of the 30–60-day anomalous cyclonic–anticyclonic circulations behave in a manner similar to that inferred from Fig. 6. These circulation migrations are not only coupled with the eastward-propagating global 30–60-day mode, but are also a reflection of the regional monsoon life cycle. The population contrast between the recurving and straight-moving tropical cyclones in Fig. 9 reflects the impact of meridional locations of the monsoon trough–ridge pattern, as well as the intensity and meridional locations of monsoon westerlies and trade easterlies. Evidently, the characteristics of tropical cyclone tracks are affected by the global 30–60-day oscillation through its modulation on the Southeast–East Asian monsoon circulation.

The composite charts of the differences in streamlines between recurving and straight-moving (Fig. 4f) tropical cyclones resemble those shown in phase 3 [maximum $\tilde{u}_W$(850 hPa) index] and phase 7 [minimum $\tilde{u}_W$(850 hPa) index], respectively. During these two phases, the anomalous circulations, both cyclonic and anticyclonic, are centered over the ocean east of Taiwan (Fig. 9). Following Fig. 9, the corresponding composite streamlines at 300 hPa are shown in Fig. 10. A comparison between these two figures reveals the *barotropic* nature of the composite 30–60-day monsoon mode by the vertically

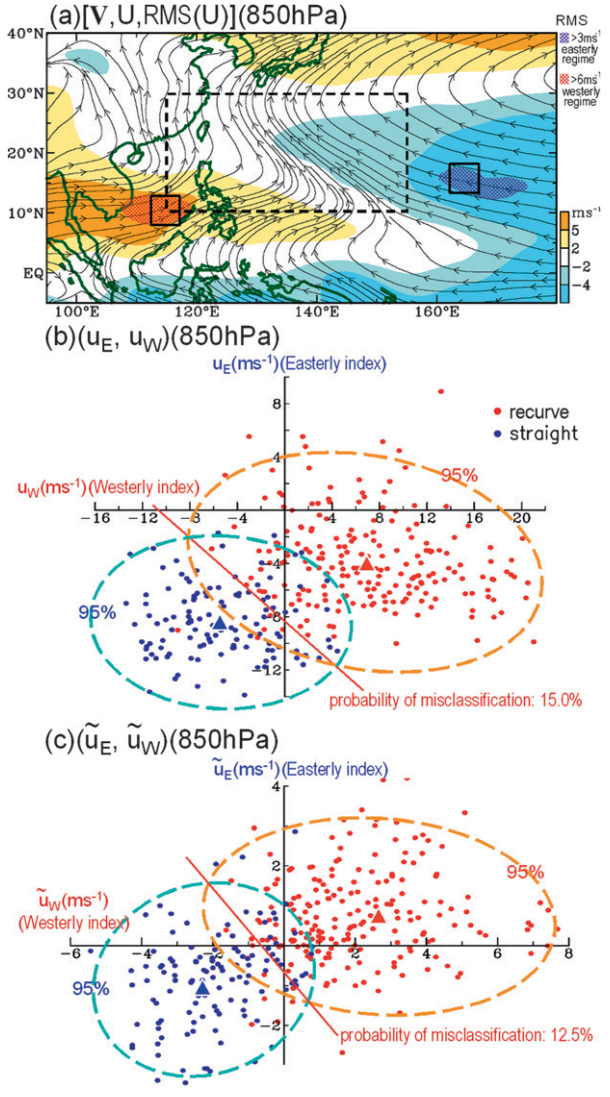

FIG. 7. (a) The climatological 850-hPa westerly (yellow–orange shadings) and easterly (blue shadings) zonal winds superimposed on streamlines for the tropical cyclone season (July–October) and a 5° × 5° square encircling the maximum rms value of the 30–60-day bandpass-filtered westerlies (red hatched) at (10°N, 115°E) and easterlies (dark blue hatched) at (15°N, 165°E). (b) A scatter diagram of the westerly index u_W (850-hPa westerlies averaged over the former square) vs the easterly index u_E (850-hPa easterlies averaged over the latter square). (c) A scatter diagram of the 30–60-day bandpass-filtered westerly index $\tilde{u}_W$ (850 hPa) averaged over the first box vs the 30–60-day bandpass-filtered easterly index $\tilde{u}_E$ (850 hPa) averaged over the second box. Tropical cyclones with their midlife positions located within the region (10°–30°N, 115°–155°E) [dashed box in (a)] were analyzed. A pair of $\tilde{u}_W$ and $\tilde{u}_E$ indices of straight-moving (recurving) tropical cyclones is marked by a blue (red) dot in (b). The averaged value of all pairs of $\tilde{u}_W$ and $\tilde{u}_E$ indices for straight-moving tropical cyclones is marked by a blue triangle, while that for recurving tropical cyclones is denoted by a red triangle. The dashed oblong covers the 95% confidence level of each group of $\tilde{u}$ indices, while the separation line (red) of bivariate normal random variables (von Storch and Zwiers 1999) is added between the two density functions. Probability of misclassification is given next to the separation line. The same procedure is applied to (c).

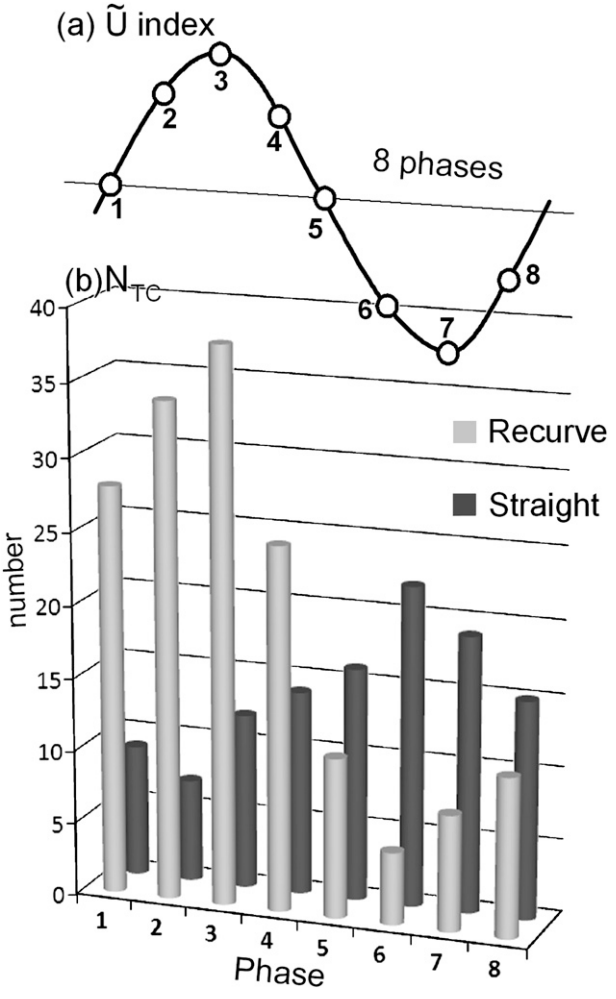

FIG. 8. (a) Schematic phase diagram of the Southeast Asian monsoon depicted in terms of the $\tilde{u}$(850 hPa) index at (10°N, 115°E), and (b) the occurrence frequency of tropical cyclones with two different tracks for every monsoon phase.

uniform anomalous circulations east of Taiwan. This barotropic characteristic of the 30–60-day anomalous circulation indicates that tropical cyclone motions are affected by not only upper-level flows, as stressed in the conventional tropical cyclone steering mechanism (see a review by Elsberry 1995), but also low-level flows.

In addition to the impact of the intensity and meridional location of monsoon westerlies and trade easterlies on the characteristics of tropical cyclone tracks, it was also observed by previous studies (e.g., Harr and Elsberry 1995a,b) that these track characteristics may be related to locations of tropical cyclogenesis through the associated large-scale anomalous circulation. However, this relationship has not been clearly shown. Genesis locations of recurving (red dot) and straight-moving (dark-blue dot) tropical cyclones are added to the composite 30–60-day bandpass-filtered 850-hPa

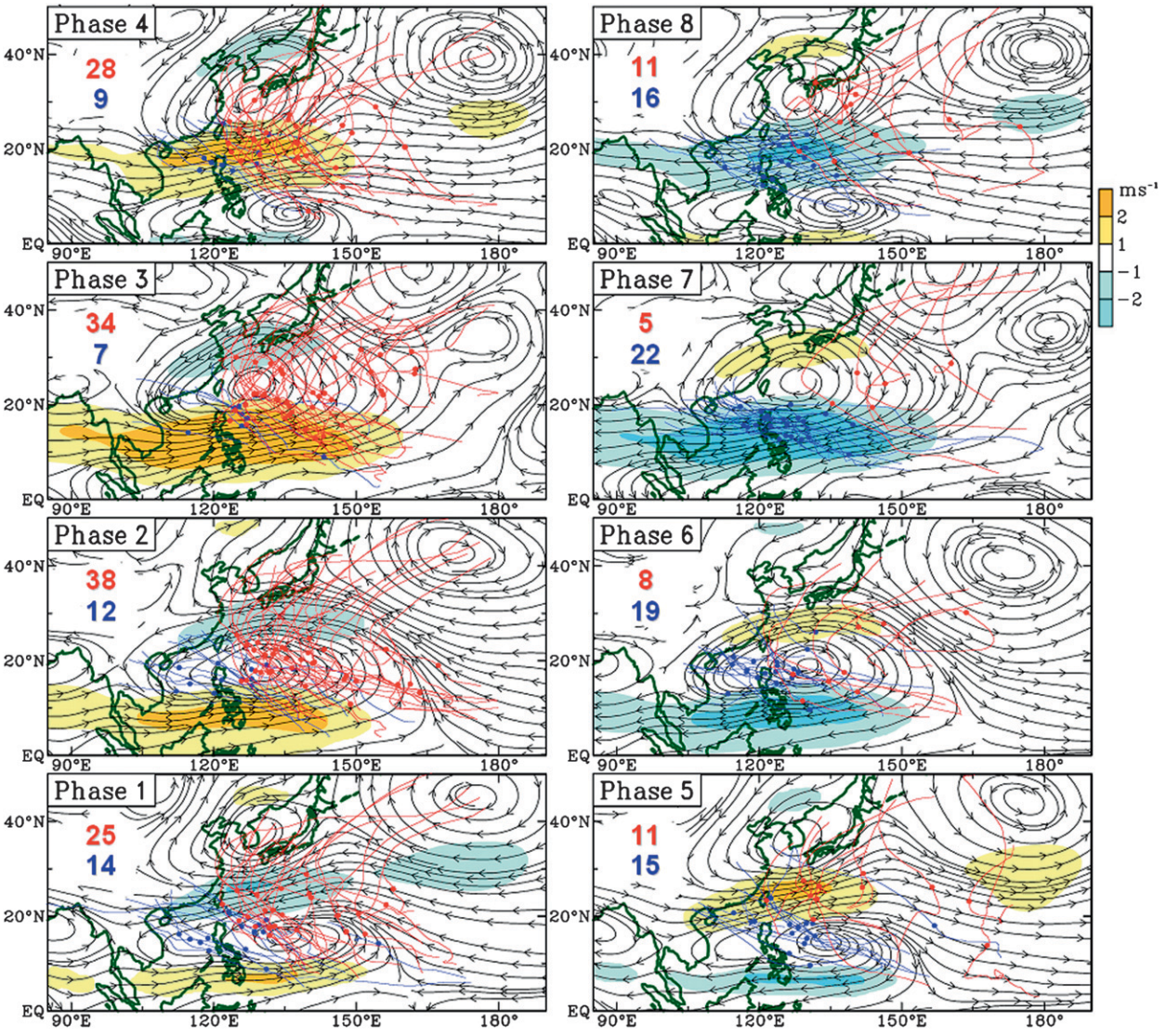

FIG. 9. Composite 30–60-day bandpass-filtered 850-hPa streamlines superimposed with the filtered westerly (easterly) zonal wind anomalies in orange (blue) for eight phases of the $\tilde{u}$(850 hPa) index defined in Fig. 10a, and midlife positions of tropical cyclones (marked by dots). Trajectories of recurving and straight-moving tropical cyclones are depicted by red and blue lines, respectively. Numbers of these two types of tropical cyclones are given in the upper-left corner of each panel, with recurving tropical cyclones indicated by the red number at the top and straight-moving cyclones by the blue number at the bottom.

streamline charts for different phases of the monsoon life cycle in Fig. 11. Comparing genesis locations during the two extreme phases of the monsoon life cycle (e.g., phase 2 versus phase 6, and phase 3 versus phase 7) reveals an east–west seesaw in genesis locations between the strong and weak monsoon phases. More recurving (straight moving) tropical cyclones develop east (west) of 140°E during strong (weak) monsoons, reflected by the intensity of monsoon westerlies. Furthermore, the northward migration of the 30–60-day monsoon trough during the strong monsoon phase facilitates the direction change of tropical cyclones formed in the vicinity of the monsoon trough. In contrast, the northward migration of the 30–60-day monsoon ridge during the weak monsoon phase hinders a northward direction change in tropical cyclones formed south of this ridge.

4. Dynamic diagnosis for changes in tropical cyclone track

In the previous section we showed how the characteristics of tropical cyclone tracks are influenced by the

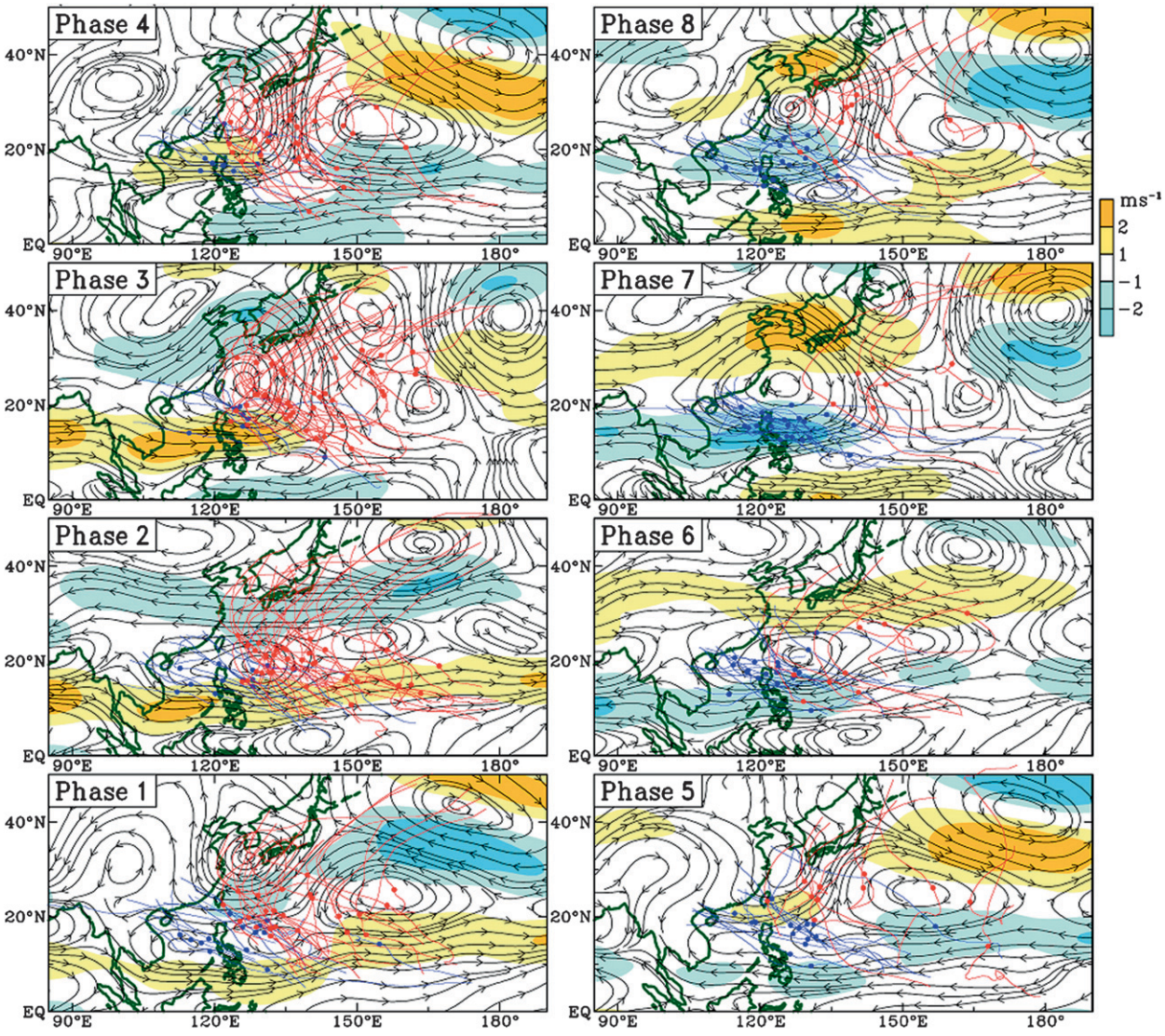

FIG. 10. As in Fig. 9, but for 300 hPa.

large-scale monsoon flow. To understand this impact dynamically, the interaction between tropical cyclones and the monsoon flow is simply examined using a vorticity budget analysis during the two extreme phases of the monsoon life cycle. However, to serve this purpose, first the basic vorticity dynamics of the monsoon flows during these two extreme phases is explained.

a. Vorticity budget of the monsoon flow

The vorticity budget equation can be expressed as

$$\zeta_t = \underbrace{-V \cdot \nabla(\zeta + f)}_{\text{VA}} \underbrace{-(\zeta + f)\nabla \cdot V}_{\text{VS}} \qquad (1)$$

$$= -V \cdot \nabla\zeta - v\beta - (\zeta + f)\nabla \cdot V. \qquad (2)$$

The notation used in this equation is conventional. For convenience, the horizontal vorticity advection and vortex stretching are denoted by VA and VS, respectively. The monsoon circulation reaches its maximum intensity in phase 3 (Fig. 12a) as reflected by the deepened monsoon trough with strong monsoon southwesterlies. Two trough lines emanate from the monsoon trough; one along the monsoon trough from the Luzon Straight to the western tropical Pacific, and another (much weaker) along the South China Sea. In contrast, the monsoon circulation reaches its breakpoint in phase 7 (Fig. 12f), as established by the subtropical anticyclone, although a newly formed monsoon trough appears in the tropics. During the active monsoon phase (phase 3), the east–west-oriented positive and negative

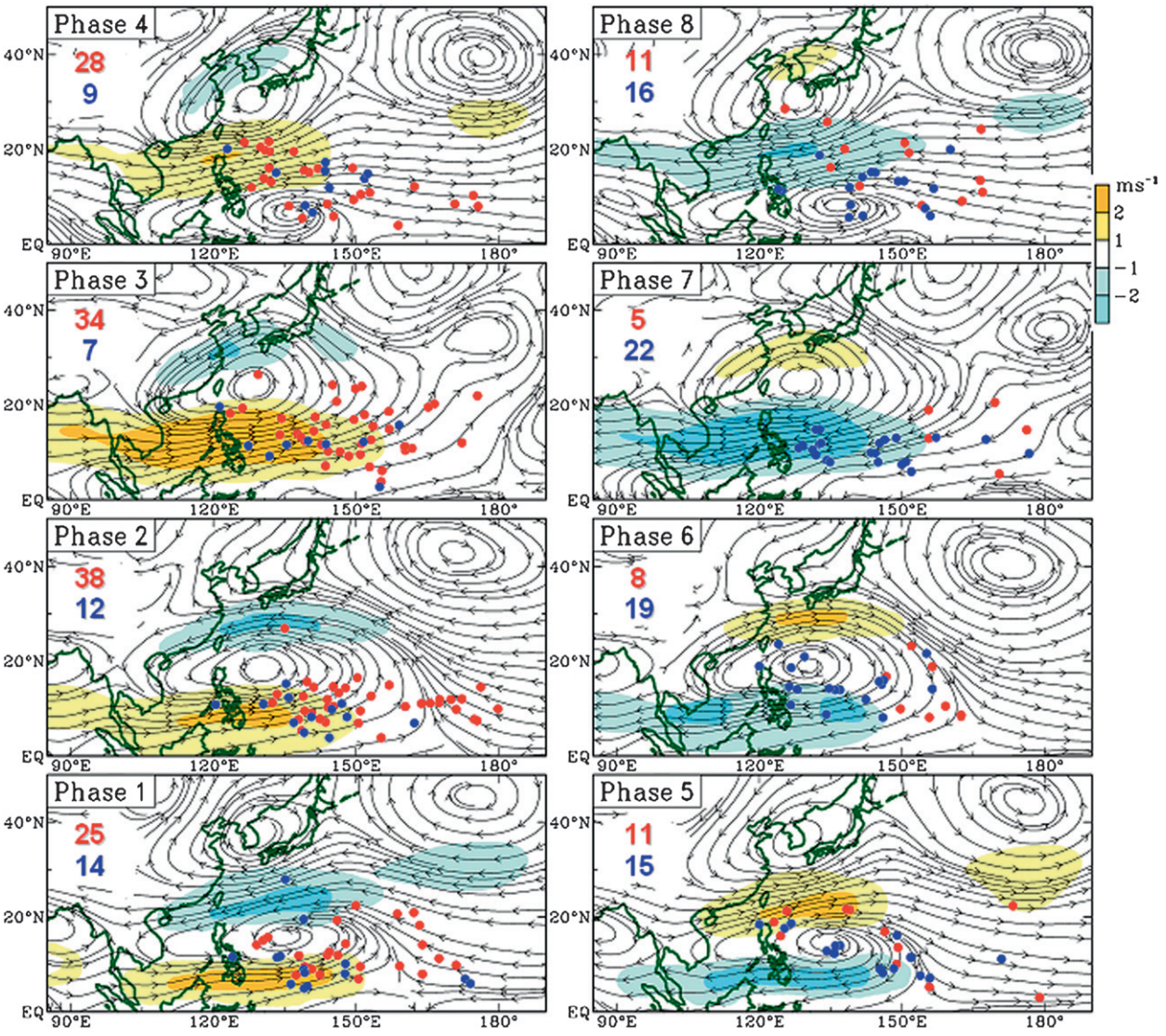

FIG. 11. As in Fig. 9, but the midlife positions of tropical cyclones are replaced by their genesis locations. For simplicity, trajectories of tropical cyclones are not shown. Genesis locations of recurving and straight-moving tropical cyclones are marked by red and blue dots, respectively.

ζ_t(850 hPa) zones are expected to be juxtaposed with the monsoon trough line, as shown in Fig. 12a. Such a ζ_t juxtaposition results in a northward propagation of the monsoon trough. The monsoon circulation over the entire region is inactive during the break phase, except in the tropics. The newly formed monsoon trough is also juxtaposed with a weak positive, east–west-oriented ζ_t(850 hPa) zone to its north and a negative one to its south. This ζ_t juxtaposition leads this new monsoon trough northward. What dynamic processes establish these well-organized east–west-oriented structures of ζ_t(850 hPa) along the monsoon trough?

Synoptically, the relative vorticity advection should be positive ahead of a trough line and negative behind the trough line. This behavior of relative vorticity advection is well depicted in Fig. 12d. Flow with smaller planetary vorticity at lower latitudes is transported northward. Thus, planetary vorticity advection is negative at the eastern end of the two monsoon troughs (Fig. 12e). Consequently, the meridional advection of the planetary vorticity functions opposite to the relative vorticity advection. Because the relative vorticity advection is generally small ahead of the trough (Fig. 12d), the VA process, a combination of these two dynamic processes, is generally negative along the monsoon flow around the trough with centers behind the trough lines (Fig. 12b). Opposite to the VA process, VS (Fig. 12c) is positive along the monsoon westerlies, with two centers

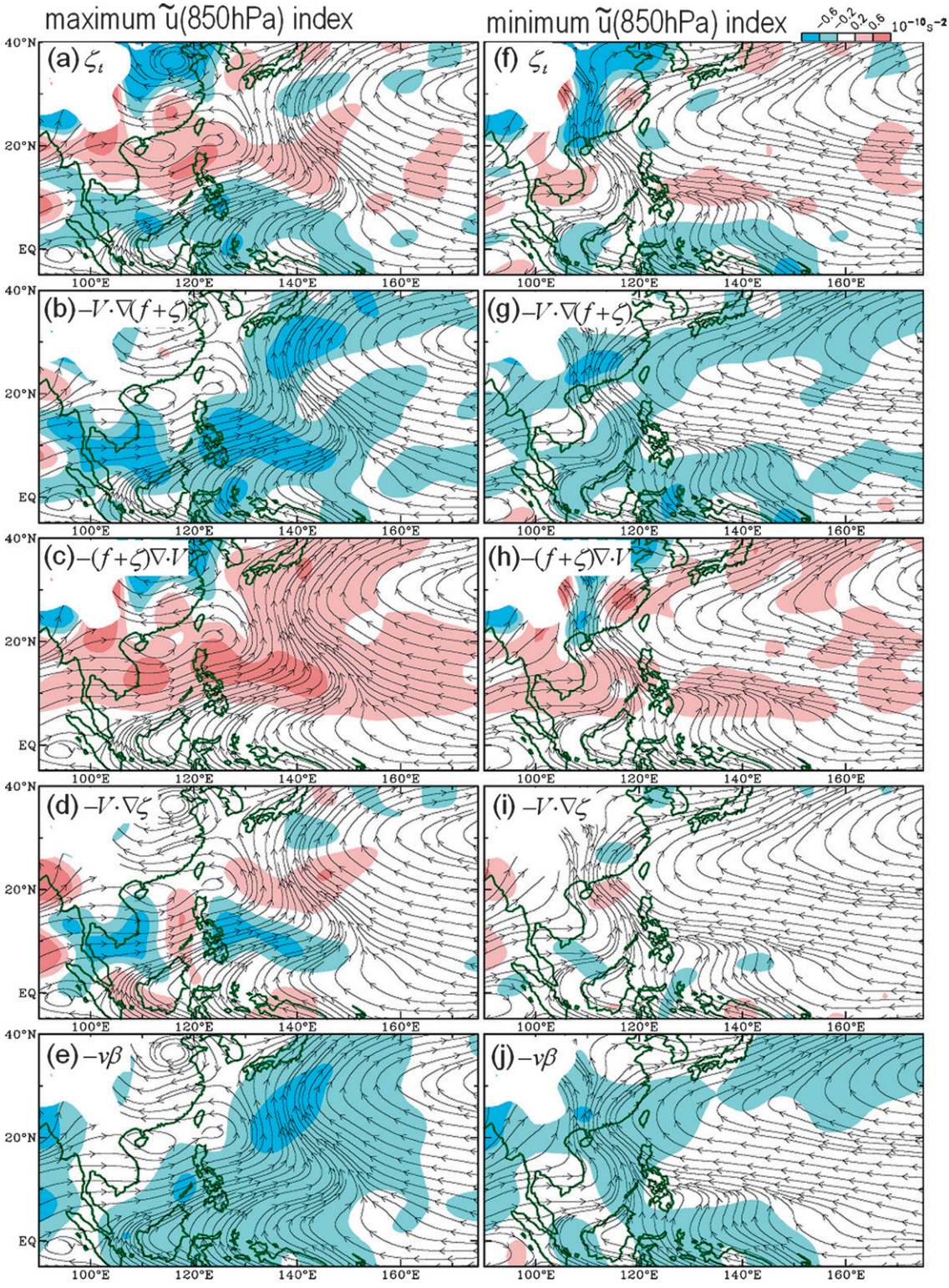

FIG. 12. Various dynamic processes included in the 850-hPa vorticity budget of the monsoon flow during the two extreme phases of the $\tilde{u}$(850 hPa) index: (a) ζ_t, (b) $-V\cdot\nabla(f+\zeta)$, (c) $-(f+\zeta)\nabla\cdot V$, (d) $-\mathrm{V}\cdot\zeta\nabla$, and (e) $-v\beta$ for the maximum $\tilde{u}$(850 hPa) phase (left column); (f)–(j) as in (a)–(e) but for the minimum $\tilde{u}$(850 hPa) phase (right column).

behind the two troughs. The northward progression of the monsoon trough is coupled with the eastward-propagating global 30–60-day mode through the local Hadley circulation (Krishnamurti and Subrahmanyam 1982; Chen and Chen 1995). Regardless of these dynamic interactions, ζ_t(850 hPa), a combination of the VA and VS processes, is characterized by a well-organized meridional juxtaposition. For the monsoon break phase, the VA (Fig. 12g) and VS (Fig. 12h) processes are active only along the southern and northern rims of the subtropical anticyclone, particularly in the tropics due to the newly formed monsoon trough. The dynamic functions of relative vorticity advection and vortex stretching along the monsoon trough revealed during the active monsoon phase are still applicable, though much weaker, to form a meridional juxtaposition of positive and negative ζ_t(850 hPa) bands (Fig. 12f).

It was pointed out at the end of section 3b that more geneses of recurving (straight moving) tropical cyclones occur east (west) of 140°E during the strong (weak) monsoon phase. This contrast of genesis locations between these two phases of monsoon circulation is consistent with the eastward extension of the monsoon trough and positive vorticity tendency ζ_t shown in Figs. 12a and 12f.

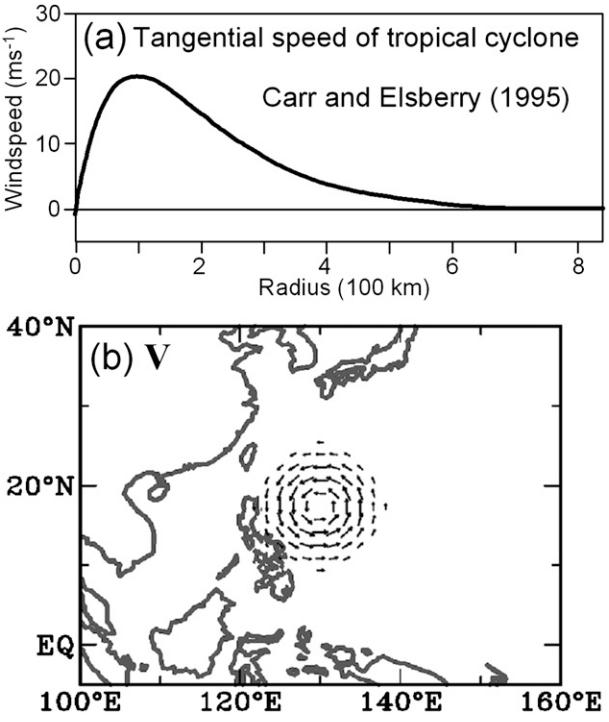

FIG. 13. Horizontal wind structure of an idealized tropical cyclone adapted from Carr and Elsberry (1995): (a) radial profile of tangential wind and (b) spatial distribution of horizontal wind vectors.

b. Interaction of a tropical cyclone with the monsoon flow

The possible direction change of tropical cyclones caused by their interaction with the monsoon flow is explored by imposing an idealized tropical cyclone on the monsoon circulation during its two extreme phases. Radial profiles of tangential wind speed (Fig. 13a), and the corresponding horizontal wind vectors at 850 hPa (Fig. 13b) of an idealized tropical cyclone used by Carr and Elsberry (1995), are adopted in our analysis. To fit the typhoon wind speed profile (Fig. 13a), the grid spacing of the ERA-40 reanalyses used for the composite streamline charts is enhanced through bilinear interpolation to 1° latitude × 1° longitude. The idealized tropical cyclone is placed at the average midlife position of tropical cyclones at (17.5°N, 135°E). The vorticity budget of the total composite flows (i.e., tropical cyclone plus environmental flow) during phases 3 and 7 of the monsoon cycle are shown in the left and right columns of Fig. 14, respectively.

After superimposing the idealized tropical cyclone to the phase-3 monsoon circulation, ζ_t(850 hPa) no longer exhibits a meridional juxtaposition of east–west-oriented positive and negative zones with the monsoon trough (Fig. 12a). Instead, the superimposed tropical cyclone alters the spatial structure of ζ_t(850 hPa) so that the positive (negative) ζ_t(850 hPa) center appears north (south) of the trough. This change in the ζ_t(850 hPa) structure may lead to the north-northwestward direction of the tropical cyclone propagation, a consequence of this dynamic interaction. The major role played by the meridional advection of planetary vorticity is primarily to generate the east–west differentiation of the vorticity tendency (Fig. 14e) and propagate the tropical cyclone westward (e.g., Chan and Williams 1987). On the other hand, the presence of a tropical cyclone during the maximum monsoon circulation phase does not change the basic characteristics of the relative vorticity advection shown in Fig. 12d, except in magnitude (Fig. 14d). Thus, the VA process shown in Fig. 14b exhibits a spatial structure similar to that during the same phase of monsoon circulation without a tropical cyclone (Fig. 12b). The VS process (Fig. 14c) is concentrated on the intensified monsoon trough in the Philippine Sea and intensifies the north–south contrast of the positive and negative ζ_t(850 hPa) contributed by the VA process.

The interaction of the idealized tropical cyclone with the weak monsoon circulation is distinctly different from its interaction with the strong monsoon circulation. Figure 14f shows that ζ_t(850 hPa) exhibits a dipole structure with a positive ζ_t(850 hPa) center west of the tropical cyclone and a negative ζ_t(850 hPa) center to its

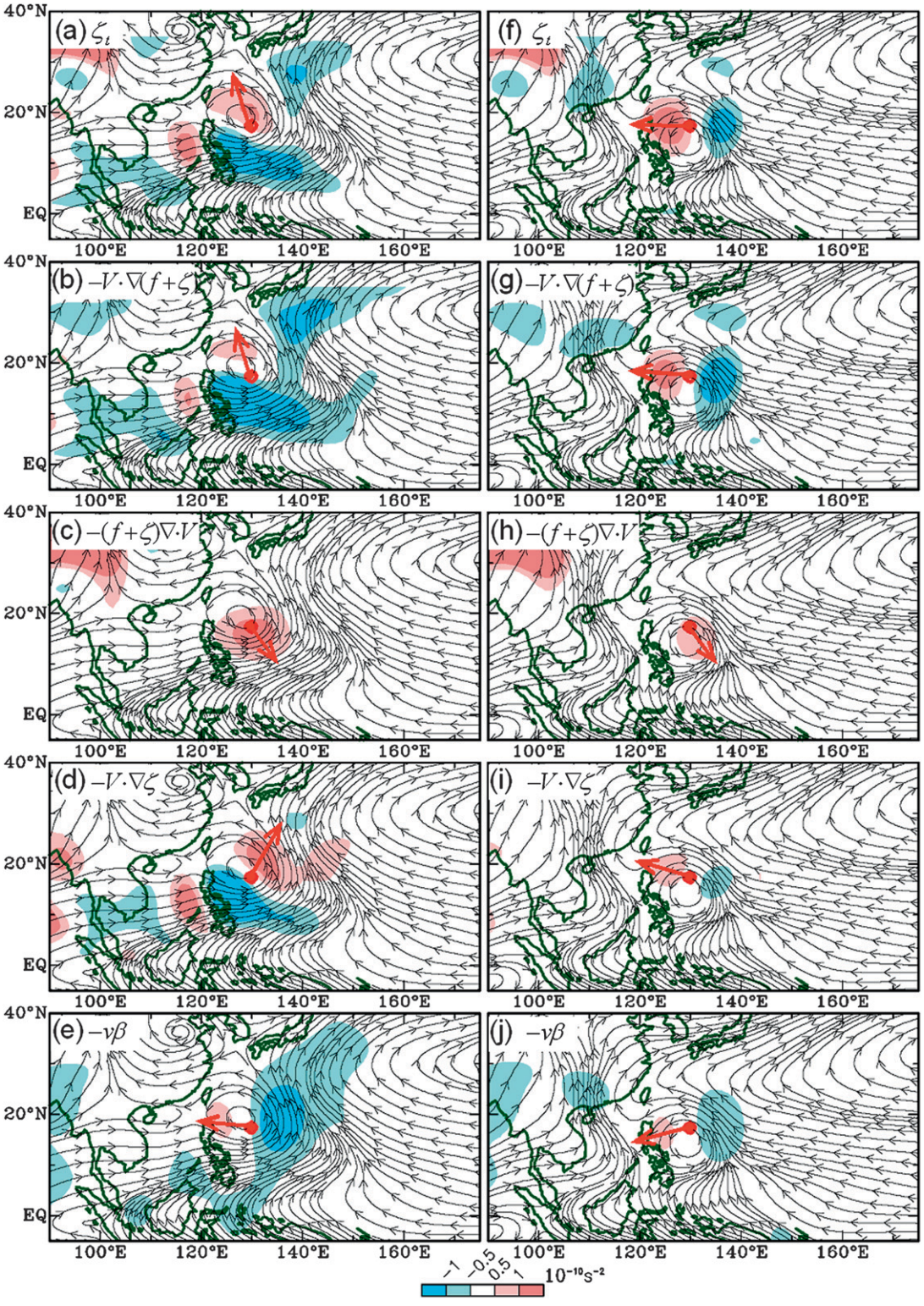

FIG. 14. Various dynamic processes included in the 850-hPa vorticity budget of the monsoon flows embedded by an idealized cyclone (depicted in Fig. 12): (a) ζ_t, (b) $-V\cdot\nabla(f+\zeta)$, (c) $-(f+\zeta)\nabla\cdot V$, (d) $-V\cdot\zeta\nabla$, and (e) $-v\beta$ during the (left) maximum $\tilde{u}$(850 hPa) phase; (right) (f)–(j) as in (a)–(e) but during the minimum $\tilde{u}$(850 hPa) phase. The scale of the vorticity tendency generated by different dynamic processes is indicated in the upper-right corner of (a). The possible moving direction of a tropical cyclone, as indicated by a red arrow in each panel, is determined by the direction from the center of the idealized tropical cyclone toward the maximum ζ_t(850 hPa).

east. This ζ_t(850 hPa) structure facilitates the westward propagation of tropical cyclones. The newly formed monsoon trough in the tropics does not seem to exert a noticeable impact on the propagation direction of tropical cyclones. The ζ_t(850 hPa) dipole is largely contributed to by VA, although VS provides a positive vorticity tendency southeast of the tropical cyclone. This positive VS may counteract or reduce the negative ζ_t(850 hPa) produced by VA east of this tropical cyclone, but it does not change the VA dipole structure. As expected, the meridional planetary advection exhibits a dipole structure (Fig. 14j) that contributes to the westward propagation of the tropical cyclone. However, without a significant contribution from the weak monsoon circulation, the relative vorticity advection primarily generated by the tropical cyclone (Fig. 14i) also exhibits a dipole structure similar to the meridional planetary vorticity advection. Both dynamic processes work coherently in the weak monsoon flow to propagate the tropical cyclone westward.

It is revealed from the vorticity budget analyses of the environmental flow shown in Figs. 12 and 14 that the tropical cyclone track can be significantly affected by its interaction with the environmental circulation. Lander (1996) observed that all tropical cyclones formed within the reverse- (SW–NE) oriented monsoon trough move northward. Earlier, Carr and Elsberry (1995) demonstrated numerically with a barotropic model that the tropical cyclone track may undergo a sudden direction change caused by Rossby energy dispersion when this tropical cyclone merges with a monsoon gyre (Lander 1994). Diagnosis of the interaction between a tropical cyclone and the monsoon circulation reveals a dynamic process that is different from that suggested by the previous study. The relative vorticity advection, a nonlinear process, sets a northeastward direction for tropical cyclone motion, while the planetary vorticity advection maintains a westward direction. The combination of these two vorticity advection processes results in a north-northwestward direction of tropical cyclone motion, but the vortex-stretching process slows this motion. Evidently, the direction change of a recurving tropical cyclone is decided by the collaborative results of all dynamic processes expressed in Eq. (1), rather than just those dictated by the horizontal vorticity advection. As inferred from this diagnosis, the difficulty in predicting the recurving tropical cyclone tracks may originate from two issues. First, forecasts of the modulation of the monsoon circulation by the global 30–60-day mode are still far from satisfactory (e.g., Hendon et al. 2000). Second, because of the lack of adequate observations over the ocean, the dynamic processes expressed in Eq. (1) may not be well depicted by the initial conditions and consequently may lead to inaccurate forecasts of tropical cyclone motion.

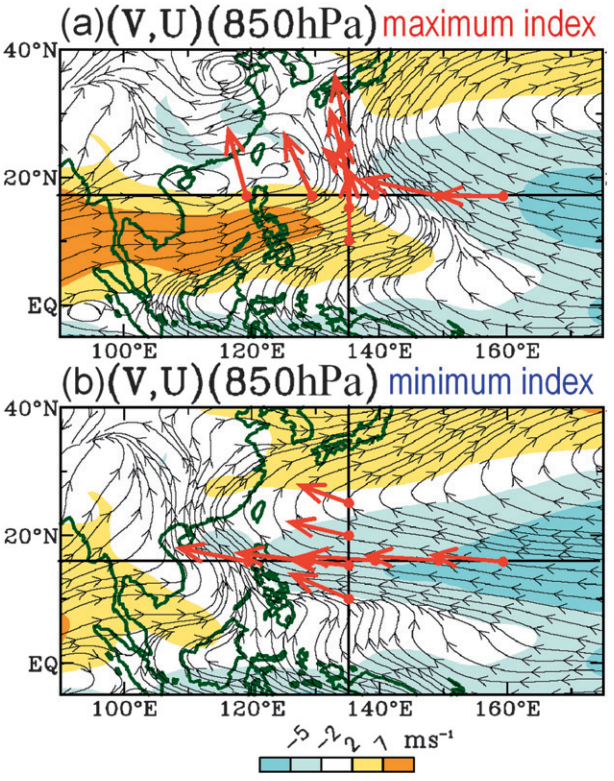

FIG. 15. The possible directions of a tropical cyclone at different longitudinal locations at 17.5°N during (a) the maximum $\tilde{u}$(850 hPa) phase and (b) the minimum $\tilde{u}$(850 hPa) phase.

The conclusion for the interaction of a tropical cyclone with the monsoon flow during its two extreme phases was drawn from an idealized tropical cyclone with a fixed location. Concern may be raised regarding the possible impacts of different tropical cyclone locations relative to the flow. It is beyond the scope of this diagnosis to clarify such concerns, but two simple diagnostic tests were performed: 1) the longitudinal location of the tropical cyclone changes from 165°E westward along the latitude of 17.5°N in a 10° interval, and 2) the latitudinal location changes from 10°N northward along the longitude of 135°N in a 10° interval. Based on the spatial structure of ζ_t(850 hPa) in the vicinity of a tropical cyclone, the possible directions of the tropical cyclone are indicated by vectors in Fig. 15 for the two extreme monsoon circulations. It is clearly shown by these tests that a tropical cyclone tends to move northward as long as it is located within the monsoon trough.

5. Conclusions

The life cycle of the Southeast–East Asian monsoon (Ramage 1952) is established by the interaction of the global intraseasonal mode with the monsoon trough and

the subtropical anticyclone (Chen et al. 2004). Previous studies (e.g., Harr and Elsberry 1991, 1995a,b) have investigated the possible impact of large-scale circulation on the characteristics of tropical cyclone tracks through the identification of anomalous circulation patterns. However, the relationship between anomalous circulation patterns and the monsoon life cycle was not the focus of these studies. In this study, an effort was made to examine the possible impact on the characteristics of tropical cyclone tracks by the intraseasonal variability of the Southeast–East Asian monsoon circulation within the context of the monsoon life cycle.

The monsoon westerlies at (15°N, 115°E) were used as a monsoon index to depict the life cycle of the South China Sea monsoon. It was observed that tropical cyclones tend to be deflected northward during strong monsoon westerlies and weak trade easterlies, and move straight northwestward when monsoon westerlies are weak and trade easterlies are strong. The former flow condition is associated with the deepened monsoon trough and the northward migration of this monsoon trough, while the latter flow condition follows the weakened monsoon trough and the northward progression of the subtropical anticyclone. The monsoon life cycle is not only reflected by the east–west seesaw of the intraseasonal oscillation between monsoon westerlies and trade easterlies, but is also regulated by northward migrations of the monsoon trough and subtropical anticyclone. The impacts on the tropical cyclone motion were illustrated with 850-hPa streamline charts during a transition period from strong trade easterlies to strong monsoon westerlies during the summer of 1996. In this transition period, the majority of tropical cyclones change from straight moving during the weak monsoon to recurving during the strong monsoon.

The changes in the characteristics of tropical cyclone tracks over the entire monsoon life cycle by the intraseasonal monsoon mode were illustrated by two different diagnostic approaches: 1) the differences in the composite environmental flows between recurving and straight-moving tropical cyclones at the midpoints of their life cycles, and 2) composites of 30–60-day modes over the entire monsoon life cycle. The major findings of these two approaches are as follow:

1) A short wave train emanating from the South China Sea along the North Pacific rim emerges from the differences in the composite streamlines between recurving and straight-moving tropical cyclones. This short wave train is characterized by a vertically uniform barotropic structure. The anomalous circulation pattern of this short wave train between Taiwan and Japan resembles that of the Pacific–Japan oscillation (Nitta 1987). The straight-moving tropical cyclones are restricted by an anomalous anticyclonic circulation centered near Taiwan, while recurving tropical cyclones are deflected northward by an anomalous cyclonic circulation.
2) Following Knutson and Weickmann (1987), a life cycle of the monsoon 30–60-day mode is divided into eight phases, with the maximum and minimum monsoon indices assigned to phases 3 and 7, respectively. The 30–60-day anomalous monsoon circulations are centered over the ocean east of Taiwan during these two extreme phases. As revealed from the 5-day composite charts centered on each phase, the population of recurving (straight moving) tropical cyclones is much larger than of straight-moving (recurving) tropical cyclones during the phases when the $\tilde{u}$(850 hPa) index was greater (less) than zero. In addition, more geneses of recurving (straight moving) tropical cyclones occur east (west) of 140°E when the monsoon index is at its maximum (minimum).

A vorticity budget analysis was performed to clarify a concern about how tropical cyclones are deflected northward by the deepened monsoon trough and intensified monsoon westerlies. It was shown that during phase 3 of the 30–60-day monsoon mode, the vorticity tendency forms positive and negative bands that are juxtaposed meridionally with the monsoon trough. This north–south juxtaposition of the vorticity tendency is intensified by the presence of a tropical cyclone to facilitate its northward propagation. In other words, the northward turning of a tropical cyclone is primarily determined by the dynamic interaction between a tropical cyclone and the monsoon trough.

The impacts of the intraseasonal variability of the monsoon circulation on the characteristics of tropical cyclone tracks were examined. A new insight regarding the relationship between the change of tropical cyclone tracks and the monsoon life cycle within the context of the intraseasonal monsoon mode was provided in this study. The preference of tropical cyclone tracks is primarily determined by the intensity of monsoon westerlies–trade easterlies in conjunction with the meridional locations of the monsoon trough and subtropical anticyclone. The relationship between the tropical cyclone motion and the monsoon life cycle offers a ''poorman's'' forecast model for the likelihood of tropical cyclone tracks during different phases of the monsoon life cycle.

Acknowledgments. This study was partially supported by the Cheney Research Foundation, NSF Grant ATM 0739326, and the NARL contract with Iowa State University through Grant NSC96-3114-P-492-002-Y.

M.-C. Yen's effort was supported by Grant NSC95-2111-M-008-016-MY3. Comments offered by Dr. Brian McNoldy and an anonymous reviewer were helpful in improving the presentation of this study. Some technical assistance provided by Paul Tsay is greatly appreciated.

APPENDIX

Tropical Cyclone Track

a. Definitions of a tropical cyclone track: Straight moving and recurving

The track of any tropical cyclone with its life cycle longer than 2 days is classified using the following approach:

1) *Straight-moving track*—A tropical cyclone track is oriented between westward and northward during its first 24 h and between westward and northwestward during its last 24 h. The track may be somewhat erratic in between these 2 days.
2) *Recurving track*—The direction of a tropical cyclone is between westward and northward during its first 24 h and between northward and eastward during its last 24 h, regardless of the track behavior in between these 2 days.

Based on these criteria, tropical cyclone tracks of these two general types over the 1979–2002 period are displayed in Figs. A1a and A1b. Our results (Fig. A1c), particularly the ratio (%) of population contrast between these two groups, are comparable with previous track groupings (e.g., Harr and Elsberry 1991).

b. Procedure for generating the average track of tropical cyclones

Locations of tropical cyclones are issued every 6 h by the JTWC. Using these locations, the gridded occurrence frequency of straight-moving (N^S_{TC}) [recurving (N^C_{TC})] tropical cyclones during the tropical cyclone seasons (July–October) of 1979–2002 [Fig. A2a (Fig. A2b)] was generated by the accumulation of all straight-moving (recurving) tropical cyclones located within a 2°-long and 2°-wide domain centered at grid points of a 2° latitude × 2° longitude grid mesh. The medians of the N^S_{TC} (N^C_{TC}) latitudinal (longitudinal) population distribution

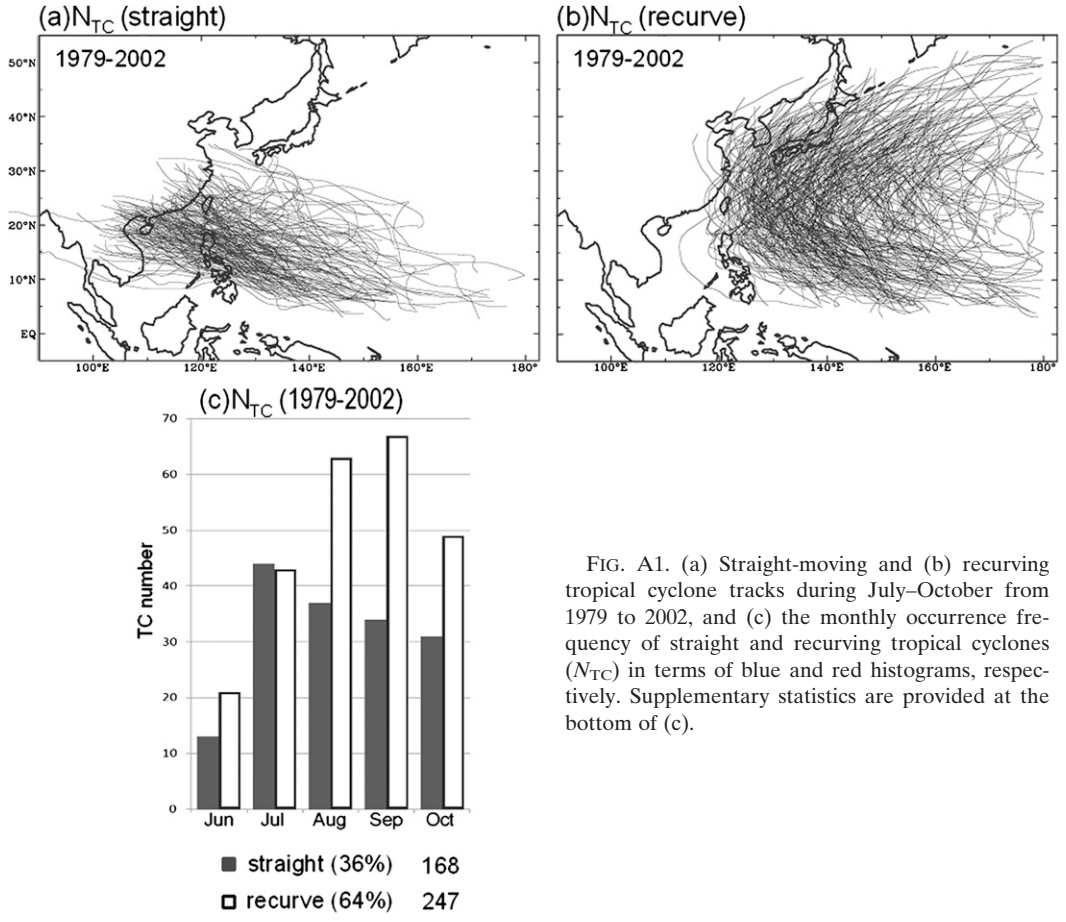

FIG. A1. (a) Straight-moving and (b) recurving tropical cyclone tracks during July–October from 1979 to 2002, and (c) the monthly occurrence frequency of straight and recurving tropical cyclones (N_{TC}) in terms of blue and red histograms, respectively. Supplementary statistics are provided at the bottom of (c).

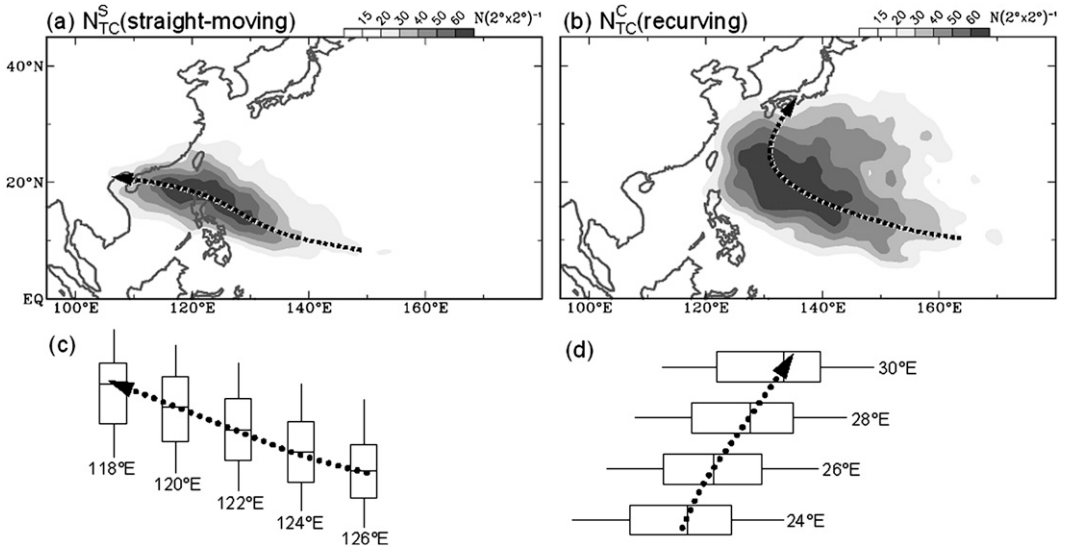

FIG. A2. Occurrence frequency of (a) straight-moving (N_{TC}^{S}) and (b) recurving (N_{TC}^{C}) tropical cyclones during July–October from 1979 to 2002, and schematic diagrams showing the boxplot of the probability distribution in the (c) latitudinal and (d) longitudinal directions. The average track for each type of tropical cyclone is indicated by a dashed arrow connecting the medians in (a) and (b).

were calculated for every 2° longitudinal (latitudinal) interval shown in Fig. A2c (Fig. A2d). The red- (blue-) dotted line connecting all medians forms the average track of straight-moving (recurving) tropical cyclones in Fig. A2a (Fig. A2b). Because the average latitude for recurving tropical cyclones to turn to a northward direction is about 24°N (Neumann 1993), the procedure in generating the average track of recurving tropical cyclones south of 24°N is the same as that of straight-moving tropical cyclones.

REFERENCES

Carr, L. E., and R. L. Elsberry, 1995: Monsoonal interactions leading to sudden tropical cyclone track changes. *Mon. Wea. Rev.,* **123,** 265–290.

Chan, J. C., and W. M. Gray, 1982: Tropical cyclone movement and surrounding flow relationships. *Mon. Wea. Rev.,* **110,** 1354–1374.

——, and R. Williams, 1987: Analytical and numerical studies of the beta-effect in tropical cyclone motion. Part I: Zero mean flow. *J. Atmos. Sci.,* **44,** 1257–1265.

Chen, L., and Y. Ding, 1979: *An Introduction to the Western Pacific Typhoons*. Science Publishing House, 491 pp.

Chen, T.-C., and J.-M. Chen, 1995: An observational study of the South China Sea monsoon during the 1979 summer: Onset and life cycle. *Mon. Wea. Rev.,* **123,** 2295–2318.

——, M.-C. Yen, and S.-P. Weng, 2000: Interaction between the summer monsoons in East Asia and the South China Sea: Intraseasonal monsoon modes. *J. Atmos. Sci.,* **57,** 1373–1392.

——, J.-M. Chen, W.-R. Huang, and M.-C. Yen, 2004: Variation of the East Asian summer monsoon rainfall. *J. Climate,* **17,** 744–762.

Elsberry, R. L., 1995: Tropical cyclone motion. *Global Perspective on Tropical Cyclones*, R. L. Ellsbury, Ed., WMO/TD-No. 693, 106–197.

Harr, P. A., and R. L. Elsberry, 1991: Tropical cyclone track characteristics as a function of large-scale circulation anomalies. *Mon. Wea. Rev.,* **119,** 1448–1468.

——, and ——, 1995a: Large-scale circulation variability over the tropical western North Pacific. Part I: Spatial patterns and tropical cyclone characteristics. *Mon. Wea. Rev.,* **123,** 1225–1246.

——, and ——, 1995b: Large-scale circulation variability over the tropical western North Pacific. Part II: Persistence and transition characteristics. *Mon. Wea. Rev.,* **123,** 1247–1268.

Hendon, H. H., B. Liebmann, M. Newman, J. D. Glick, and J. E. Schemm, 2000: Medium-range forecast errors associated with active episodes of the Madden–Julian oscillation. *Mon. Wea. Rev.,* **128,** 69–86.

Holland, G. J., 1983: Tropical cyclone motion: Environmental interaction plus a beta effect. *J. Atmos. Sci.,* **40,** 328–342.

Kanamitsu, M., W. Ebisuzaki, J. Woolen, S.-K. Yang, J. J. Hnilo, M. Fiorino, and G. L. Potter, 2002: NCEP/DOE AMIP-II Reanalysis (R-2). *Bull. Amer. Meteor. Soc.,* **83,** 1631–1643.

Knutson, T. R., and K. M. Weickmann, 1987: 30–60 day atmospheric oscillations: Composite life cycles of convection and circulation anomalies. *Mon. Wea. Rev.,* **115,** 1407–1436.

Krishnamurti, T. N., and D. Subrahmanyam, 1982: The 30–50 day mode at 850 hPa during MONEX. *J. Atmos. Sci.,* **39,** 2088–2095.

Lander, M. A., 1994: Description of a MG and its effect on the tropical cyclones in the western North Pacific during August 1991. *Wea. Forecasting,* **9,** 640–654.

——, 1996: Specific tropical cyclone track types and unusual tropical cyclone motions associated with a reverse-oriented monsoon trough in the western North Pacific. *Wea. Forecasting,* **11,** 170–186.

Madden, R. A., and P. R. Julian, 1971: Detection of a 40–50 day oscillation in the zonal wind in the tropical Pacific. *J. Atmos. Sci.,* **28,** 702–708.

——, and ——, 1972: Description of global-scale circulation cells in the tropics with a 40–50 day period. *J. Atmos. Sci.,* **29,** 1109–1123.

Murakami, M., 1979: Large-scale aspects of deep convective activity over the GATE area. *Mon. Wea. Rev.,* **107,** 997–1013.

Neumann, C. J., 1993: Global overview. *Global Guide to Tropical Cyclone Forecasting*. G. J. Holland, Ed., WMO/TC-No. 560, Rep. TCP-31, 1–43.

Nitta, T., 1987: Convective activities in the tropical western Pacific and their impact on the Northern Hemisphere summer circulation. *J. Meteor. Soc. Japan,* **65,** 373–390.

Ramage, C. S., 1952: Variation of rainfall over south China through the wet season. *Bull. Amer. Meteor. Soc.,* **33,** 308–311.

Uppala, S. M., and Coauthors, 2005: The ERA-40 reanalysis. *Quart. J. Roy. Meteor. Soc.,* **131,** 2961–3012.

von Storch, H., and F. W. Zwiers, 1999: *Statistical Analysis in Climate Research*. Cambridge University Press, 528 pp.